
Interpretation of potential field data in the area of the Loppa High, Western Barents Sea, Norway

C. Barrère

Geological Survey of Norway (NGU)¹

Norwegian University of Science and Technology (NTNU)²

J. R. Skilbrei

Geological Survey of Norway (NGU)¹

Abstract: We present a preliminary 2D model of a combined gravity and magnetic field interpretation of the Loppa High in the SW Barents Sea. The advantage of our modelling approach allow us to distinguish features pertaining to the nature of the basement, which is not possible using only the gravity field. Our model is constrained by seismic profiles, well logs, petrophysical measurements, and core samples. The Euler Deconvolution Solutions (EDS) are commonly computed to estimate the depth to magnetic sources. In our context, this method has revealed two very interesting features. Plotted EDS on a map allows us to follow alignments of tilted blocks occurring in parallel bands; and plotted EDS along 2D profiles enables us to outline the changes in magnetic properties within the basement in the Loppa High.

Below the Bjørnøyrenna Fault Complex (BFC), which marks the northwestern boundary of the Loppa High, we have to include high-density material. Combined with the inferred existence of a detachment below the BFC, the model has helped to depict what could be a gneiss dome. The extension of that structure could fit the gravity anomaly that exists between the BFC and the Loppa High.

Based on petrophysical measurements of rocks outcropping onshore in northern Norway, the magnetic modelling highlights the Precambrian basement as the main source of the magnetic anomalies. The Precambrian basement units are characterised by magnetic susceptibility values from 0.010 (SI) to 0.080 (SI) and a remanence of 0.550 A/m. In this area, the Fennoscandian Shield is mainly covered by Caledonian nappes that locally reach up to 5 km in thickness (*Olesen et al., 1990; Sigmond, 1992*). Even if their magnetic properties are representative, with magnetic susceptibility values of 0.072 (SI) and a remanence of 0.0397 A/m, their abundance is not sufficient to act as significant magnetic source. The modelling also shows that the magnetic anomalies within the Precambrian basement in the Loppa High reflect its buried 'hilly topography' that is an erosion unconformity.

¹ Leiv Eirikssons vei 39, 7491 Trondheim, Norway

e-mail: cecile.barrere@ngu.no; jan.skilbrei@ngu.no

² 7491 Trondheim, Norway

Key words: gravity anomaly, magnetic anomaly, seismic data, Barents Sea, 2D modelling, Euler deconvolution, basement and gneiss dome.

1. Introduction

The Barents Sea Shelf is located in the northernmost Europe and extends from the North Atlantic and Svalbard archipelago in the west to Novaya Zemlya in the east, over a distance of 1000 km. In the west and north the Barents Sea is bounded by its Cenozoic passive margins. The Barents Sea is divided into the Eastern Barents Sea, showing long-wavelength basins, and the Western Barents sea that is characterised by typical rift basins (*Doré and Gage, 1987; Ziegler, 1988; Doré, 1991*). Our study area is located in the SW Barents Sea and limited to 71°N – 75°N and 13°E – 32°E (Fig. 1), encompassing major structural highs and lows in the basement.

In the area, sedimentary rocks in the basins range in age from Late Palaeozoic to Quaternary. Locally, the successions in the basins have a thickness of more than 14 km.

The Loppa High is surrounded by individual faults or fault complexes that were active during the formation of this positive basement feature (*Gabrielsen et al., 1990; Skilbrei, 1995*).

Our study has aimed at characterising the basement underlying the deep basins and understanding the relationships between structural highs and lows and the deep crustal configuration. To do this, we have extended geological units from the land into the sea areas, using geophysical data sets and rock properties such as density, magnetic susceptibility and remanence to constrain our interpretation. The potential field data, such as gravity and magnetic data, provide an idea of mass and magnetic susceptibility distribution in the crust. Short-wavelength and long-wavelength information are contained in each data set, allowing the investigation of deeply buried geological features such as basement rock distribution and Moho topography.

Magnetic anomalies of regional significance can be related to Precambrian, mafic and felsic, high-grade metamorphic rocks. These two types of units are characterised by different ranges of susceptibilities, which allows them to be distinguished. In contrast, intrasedimentary sources give high-frequency anomalies.

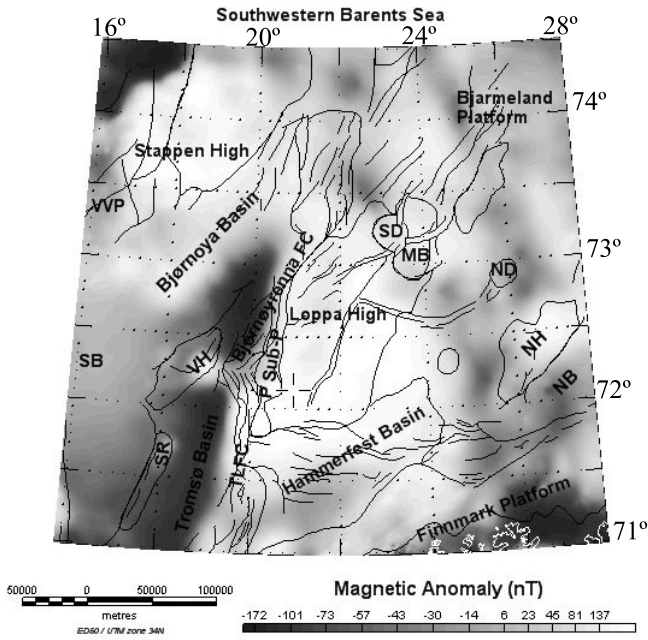


Fig. 1. Location map: VVP = Vestbakken Volcanic Province; SB = Sørvestsnaget Basin; VH = Veslemøy High; SR = Senja Ridge; SD = Svalis Dome; MB = Maud Basin; ND = Norvarg Basin; NH = Norsel High; NB = Nordkapp Basin. The coast of Finnmark is visible in the southeast corner (white solid line). The black solid lines represent faults, the outline of structural highs and lows, and the platform areas.

Although a lot of industrial seismic data are available, the complex structure of the Loppa High is yet to be revealed. To study the Loppa High, we perform the Euler Deconvolution Solutions (EDS) calculation and 2D modelling along a profile starting in the Bjørnøya Basin, crossing the Bjørnøyrenna Fault Complex and the Loppa High, and finishing on the Bjarmeland Platform. The model is constrained by seismic, well logs, petro-physical measurements and core samples. This 2D model is adjusted simultaneously to the magnetic and gravity anomalies.

By comparing the 2D modelling with the EDS we can deduce ways of improving the model; for example, introducing basement rocks in tilted blocks and confirming the locations of magnetic property changes within the basement rocks.

2. Databases

For the Western Barents Sea, NGU holds gravity, magnetic and petrophysical databases. Statoil provides seismic profiles and well logs, when these are not available from the Norwegian Petroleum Directorate.

2.1. Magnetic data

Aeromagnetic data (Fig. 2) are available from aeromagnetic airborne surveys carried out by the Norwegian Geological Survey (NGU) and described in *Olesen et al. (1997)*. Because we are interested in investigating the deep crustal sources, we upward continued the magnetic field to 600 m, using the routines available in the Geosoft software (*Geosoft, 2006*). Upward continuation is considered a robust technique (e.g. *Nabighian et al., 2005*), and

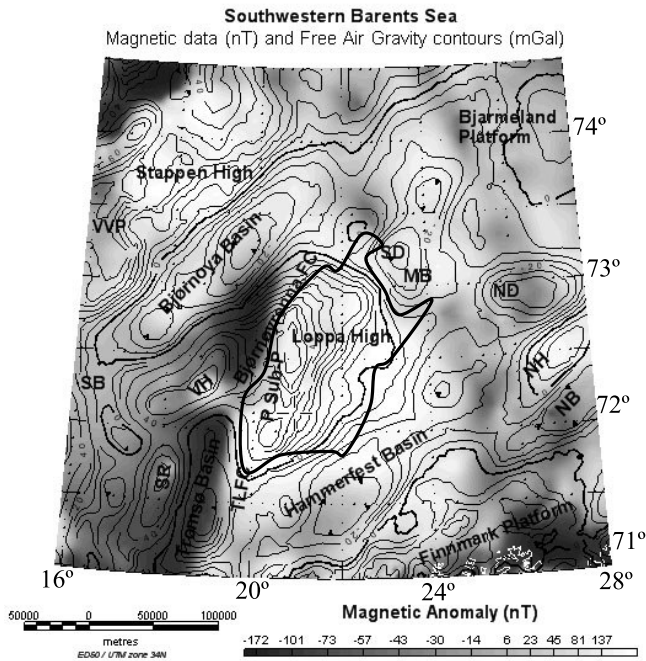


Fig. 2. Overlay of magnetic data set shown in shades of grey, gravity data contours (contour distance = 5 mGal) and the outline of the Loppa High tectonic unit (inside thick solid line).

it leads to suppression of short wavelengths and, thus, a relative accentuation of the long wavelengths associated with the basement. The data are adjusted to the International Geomagnetic Reference Field (IGRF).

2.2. Gravity data

Gravity data are available from the compilation presented by *Skilbrei et al. (2000)*. On land, the compilation consists of terrain-corrected Bouguer anomaly values computed using a rock density of 2670 kg/m^3 . Offshore, free-air anomalies are used. Distances between the gravity stations are highly variable, but range generally from 1 km to 10 km. A grid cell size of 1 km by 1 km was used in the compilation. To level the surveys, the International Gravity Standardisation Net (IGSN 71) and the Gravity formula 1980 for normal gravity were used. Fig. 2 shows the gravity contours.

As regards the potential field (Fig. 2), two provinces can be distinguished within the Loppa High. The western part of the high is characterised by a free air gravity anomaly high and magnetic anomaly low, whereas the eastern part is marked by a free air gravity anomaly low and a magnetic anomaly high.

2.3. Accuracy of the data used

Several geophysical data sets have been processed and described (*Olesen et al., 1997; Skilbrei et al., 2000*). The accuracy of the data depends on many parameters including line distance, instrumentation, positioning and acquisition systems, processing, and weather conditions during the survey period. The accuracy of the onshore gravity is determined by the accuracy of the gravity corrections, point distance, instrumentation, and accuracy of the x, y and most critically the z-coordinate. In general, the accuracy is within 1 mGal. The shipborne gravity varies in quality because many different surveys and data sets have been included in the final processing data; however, most lines are better than 1 mGal, after a smoothing of the 'point-shadow' and application of a 3 km low-pass, cut-off filter. The noise envelope of the aeromagnetic profile data varies between 4 to 5 nT (oldest data) to better than 0.1 nT. The profile distance is from 1 km to 8–10 km over the greater parts of the study area. During survey periods,

special attention was paid to the magnetic time variations although a direct subtraction of the base magnetometer data from the survey data was not performed because of the large distances involved (e.g. *Skilbrei, 1991*). Fortunately, the Loppa High is covered with relatively modern data from the 1980s, when precise radio positioning systems and modern proton magnetometers were used. Within the study area, the potential field sources are located at depths great enough to prevent aliasing of anomaly data during interpolation between lines and gridding. The only exception to this is the shallow bathymetry and the Quaternary strata which do not produce significant anomalies.

2.4. Seismic and petrophysical information

Information about the regional structure of the crust is available from published models based on Ocean Bottom Seismometer (OBS) data (*Breivik et al., 1998, 2002, 2003*). In addition, we had access to depth-converted, industrial seismic-reflection profiles that allowed a detailed interpretation of the upper crustal structures along our modelled profile.

Information about the density distribution in the sedimentary basins was obtained from *Tsikalas (2002)*, and magnetic susceptibilities and remanence values from NGU databases (*Olesen et al., 1990*). The rock samples were sampled in the Finnmark, northern Norway, the closest onshore area to the Loppa High. For each rock type average values of density, susceptibility and remanence were computed and used as initial values for the modelling. However, we are aware that metamorphic rocks are very heterogeneous. We have also used petrophysical graphs from the existing literature (*Olesen et al., 1990; Skilbrei et al., 1991*).

2.5. Integration of structural elements and the potential field maps

We have integrated the positions of the faults with the free air gravity field (Fig. 3a) and magnetic field (Fig. 3b) data sets in order to investigate the regional distribution of the anomalies. Several of the tectonic units in the study area present a clear gravity signature; the Stappen High, the Veslemøy High and the Senja Ridge are quite well delimited by gravity data.

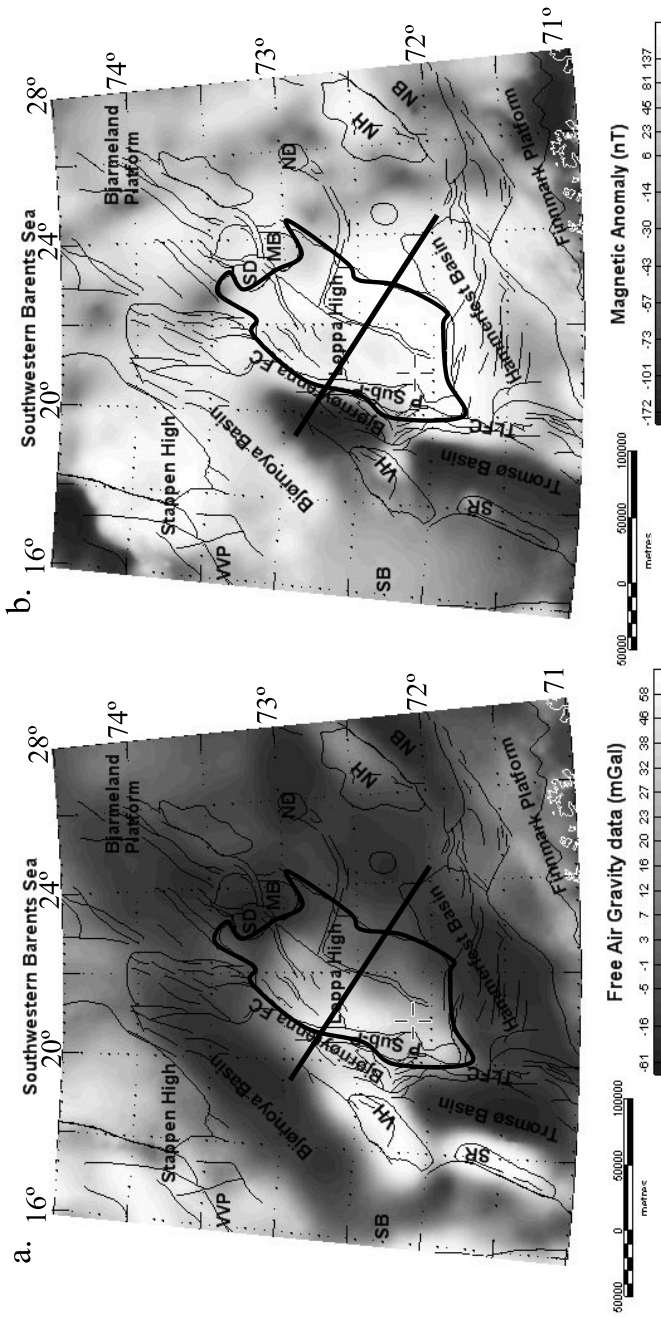


Fig. 3. Integration of faults and potential field data; the Loppa High tectonic unit is outlined by a thick black line (from geophysical data). The modelled profile is located by straight solid lines. VVP = Vestbakken Volcanic Province; SB = Sørvestnaget Basin; VH = Veslemøy High; SR = Senja Ridge; SD = Svalis Dome; MB = Maud Basin; ND = Norvarg Basin; NH = Norsel High; NB = Nordkapp Basin.

The Norsel and the Gardabanken Highs, as well as the Bjarmeland and the Finnmark Platforms, present medium gravity anomalies. The case of the Loppa High is somewhat peculiar as a gravity anomaly of 60 mGal is focused along the Bjørnøyrenna Fault Complex striking roughly N–S, which does not accord with the tectonic unit established by seismic interpretation. Gravity lows between –30 mGal and –55 mGal underline the Tromsø, Hammerfest, Bjørnøya, Maud, Nordkapp and Sørvestsnaget basins, as well as the Svalis and Norvarg Domes.

The magnetic field (Fig. 3b) does not fit the tectonic units because it is more complex than the gravity field. Indeed, the magnetic field reflects a combination of top basement topography and intrabasement sources. It is notable that the Loppa High and the Stappen High, known to be basement highs, present strong magnetic anomalies (from 100 nT till 900 nT). Some magnetic anomalies seem to be clearly limited in space, like those in the northern part of the Norsel High, the Senja Ridge and the Veslemøy High. The Hammerfest Basin presents a medium magnetic anomaly (from –15 nT to 60 nT) that is more intense in the eastern part, at the junction of three fault complexes: the Finnmark, the Asterias and the Nysleppen Fault Complexes. It is also notable that the salt signatures of the Svalis (90 nT) and the Norvarg Domes (15 nT) create positive magnetic anomalies, and the gravity low anomalies found at the location of the Maud Basin and the faults striking NE–SW in the north of the Maud Basin correlate with high-magnetic anomalies. In addition, we must mention that the Sørvestsnaget Basin has quite a high magnetic anomaly for a sedimentary basin of at least 12 km thickness.

3. Euler deconvolution

3.1. Euler's solutions computation

The Euler homogeneity relation describes the behaviour of the field created by a source to the point of measurement (*Thompson, 1982*):

$$(x - x_0) \frac{\partial \Delta T}{\partial x} + (y - y_0) \frac{\partial \Delta T}{\partial y} + (z - z_0) \frac{\partial \Delta T}{\partial z} = N(B - T)$$

Where x_0 , y_0 and z_0 is the position of the magnetic source we want to determine.

T is the total field measured at (x, y, z) , and B is the regional magnetic field.

N is the degree of homogeneity, interpreted as a Structural Index (SI), actually a measure of the rate of change with distance of the field (*Thompson, 1982*). Choosing the correct SI causes the desirable focusing of Euler Deconvolution solutions (*Reid et al., 1990*).

An “Euler Window Computation” determines an area of grid data; the relevant size is chosen when it is large enough to include substantial variations of both the field and the field gradients but small enough not to incorporate effects from multiple sources. The uncertainty is mainly the result of a window containing no significant gradient or including gradients arising from several sources. In addition, there exist several possibilities to window the results based on the statistics of the solutions.

3.2. Interpretation of Euler solutions distribution

The EDS computed using Geosoft software (*Geosoft, 2006; Reid et al., 1990*) estimate the depth to magnetic sources. Investigating for contacts ($SI = 0$) and a Window Size (WS) of 20 km the computation of EDS allows us to highlight several geological provinces (Fig. 4). Two zones presenting a large cluster of solutions at 2500 m depth are surrounded by zones of low EDS density. From the overlay of the structural elements and the magnetic data, we notice that areas of the Loppa High and the Stappen High areas correspond to the high-clustered provinces. Some solutions are plotted directly above the basement faults of Bjørnøyrenna, forming alignments, at depths in excess of 3300 m; they draw a boundary between the high and the basins. The Loppa High is delimited by alignments of solutions along two parallel segments along its west side.

All EDS less than 5 km away from the profile are then extracted, stored and plotted over the geological model. This is described next.

4. Potential field modelling

The GM-SYS modelling program calculates the gravity and magnetic response from a geological model defined using known rock properties (*Blakely*

and Connard, 1989; Blakely, 1995; Campbell, 1983, Geosoft, 2006). We extract a profile from the free-air anomaly grid and the magnetic grid. As a background, we display a seismic bitmap and other depth-scaled information (e.g., well logs). The overlays permit us to constrain the geological model, which is in 2D. After fixing the layer structure we apply petrophysical parameters to each layer: density, susceptibility and remanence. Rapid calculation of the gravity and magnetic response allows quick testing of alternative solutions. Extracted from the database and computed for a certain SI and Window Size (WS), the EDS can then be plotted over the seismic bitmap and the geological model.

The modelled Profile 1 (see location in Figs 3 and 4) starts in the middle of the Bjørnøya Basin, crosses the Bjørnøyrenna Fault Complex and the

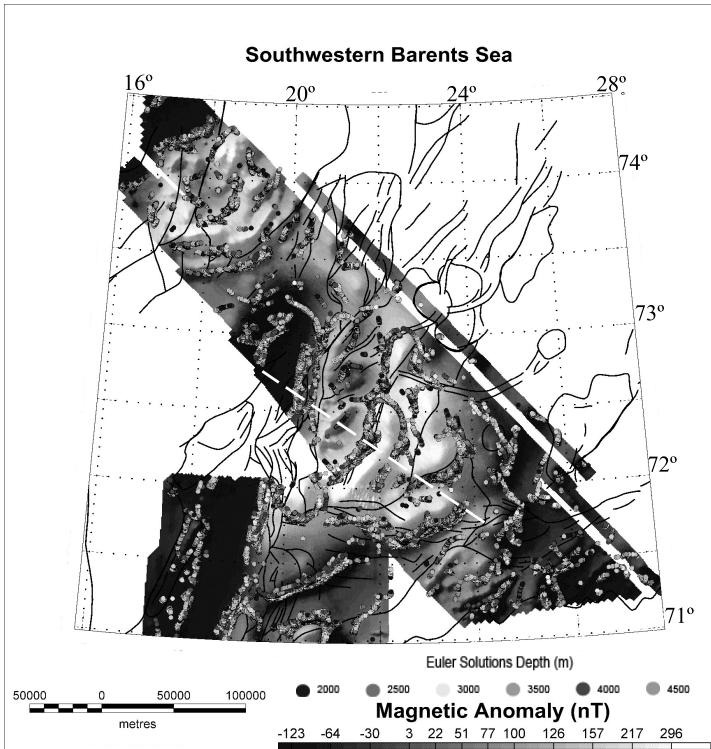


Fig. 4. Overlay of high-quality magnetic field data (cell size = 1000 m, flight “height” = 600 m), Euler Deconvolution Solutions (SI = 0, WS = 20 km). The modelled profile is marked by a straight dashed line.

whole Loppa High and ends on the Bjarmeland Platform. The main geometry is based on the reflectors observed on the seismic section as the Base Quaternary, Base Tertiary, intra Upper Cretaceous, intra Lower Cretaceous, Base of Upper Jurassic, Top Triassic, near Top Permian, near Top Basement and Top Basement as recognised in the seismic interpretation published by *Gabrielsen et al. (1990)*. For the deepest part we use the OBS models published by *Brevik et al. (1998, 2002 and 2003)*.

A first-order feature is a huge gravity anomaly located along the Bjørnøyrenna Fault Complex and the Tromsø-Loppa Fault Complex. The anomaly strikes parallel to the faults and has an elliptical shape (Fig. 3a). In this area, there is also a magnetic anomaly, but this seems to be part of the main anomaly linked with the basement topography. Before modelling the potential field data we must study carefully the structural information available. This is a key step for the reliability of any future model.

After the geometry has been set up, we apply densities to all layers; then magnetic susceptibility and remanence to the basement and lower crustal blocks, considering them as the two sources of the magnetic signal. Because the Curie temperature is 580°C for magnetite, we can limit the extension of potential magnetic sources to the crustal material and assume it to be non-magnetic below the Moho (*Clark, 1966*). Also, the sediments are relatively non-magnetic (*Clark, 1966*).

4.1. Gravity modelling

For the density structure we apply a density of 3300 kg/m³ to the Mantle, 2900 kg/m³ to the Middle Crust and 3000 kg/m³ to the Lower Crust (from the 3D seismic velocity model of *Bungum et al., 2005*). To fit the observed field we had to use two density values for the crystalline rocks of the basement crust; indeed, we used mainly 2700 kg/m³ but we raised this value to 2750 kg/m³ for a median block within the Loppa High. For the sediments we use a density range from 1900 kg/m³ to 2650 kg/m³ (*Tsikalas, 1992*), depending on the age and burial depth of the layer (Fig. 5).

We observed that the Moho depth varies along the profile from 25 to 32 km. From the Moho map of *Bungum et al. (2005)* and the OBS data published by *Brevik et al. (2002)*, we started with a Moho depth of around

35 km. Under the Bjørnøya Basin area a shallower Moho depth is needed to model the gravity field value (Fig. 5).

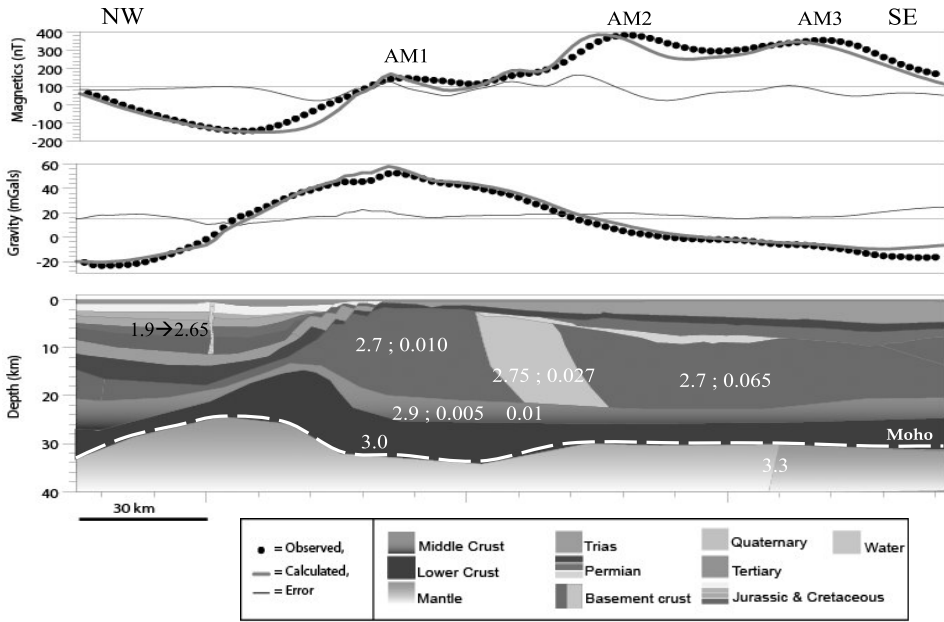


Fig. 5. Modelling along Profile 1. The shallow part is constrained by the seismic reflection interpretation, and the Moho depth by the surrounding OBS data. Middle and Lower Crust convexity and distinction between basement blocks are linked to the potential field interpretation. Note that the water layer and the different sedimentary layers used in the forward model (the densities vary between 1.9 and 2.67 g.cm³ based on borehole information) are not shown.

4.2. Magnetic modelling

The fit of the modelled magnetic anomaly to the observed anomaly is not as good as for the gravity field. However, the focus was on the modelling of the gradient of the magnetic field and not to model the amplitude perfectly, since the gradient is most sensitive to the depth of the magnetic sources.

Using mean values computed from the NGU database, the remanence is fixed at 0.551 A/m within the Basement Crust of the Precambrian age. For

the magnetic structure, the Precambrian basement is split into three blocks, using susceptibility values of 0.010, 0.027 and 0.065. A susceptibility value is applied to the Middle Crust but its value can be from 0.005 to 0.010 without having a big impact on the modelled magnetic curve (Fig. 5).

This preliminary modelling of the three magnetic anomalies AM1 (150 nT), AM2 (385 nT) and AM3 (355 nT) along Profile 1 shows that a distinction between three Precambrian lithologies can help to explain the potential field anomalies (Fig. 5). The top basement topography seems to be of high importance, as well. Indeed, it seems that the shape of the AM2 and AM3 anomalies correlate with the top basement undulation.

The overlay of the extracted EDS plotted less than 5 km from the Profile 1 (SI = 0, contact underlined; WS=20 km) gives a vertical distribution in the middle of the basement block. This distribution confirms the change in magnetic properties, forcing us to distinguish two different lithologies within the basement (Fig. 6).

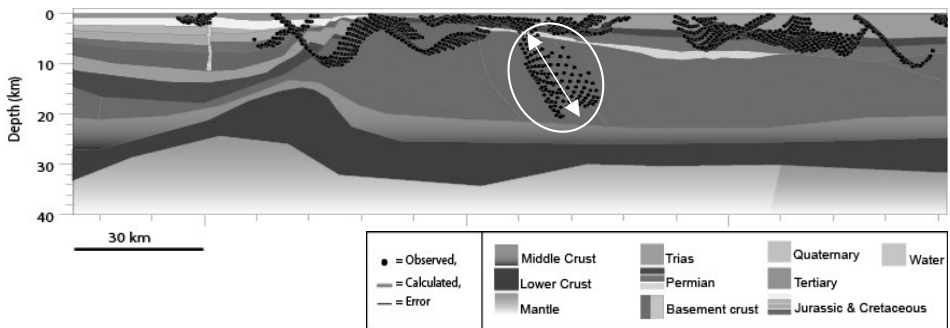


Fig. 6. Display of the EDS over the geological model. The groups of shallow solutions are not interpreted because they are located in the sediments and/or are artifacts created by the projection of the EDS from the sides.

5. Interpretation and discussion

Because of the reduced seismic data quality in the basins surrounding the Loppa High and an unclear limit between basement rocks and Late Palaeozoic sediments on the Loppa High itself, we had to interpret the top

basement mainly from the potential fields. In order to model the pronounced gravity and magnetic curves along the profile, we estimate the depth to the top of the basement at around 3 km.

Comparing the seismic image and the location of the two alignment plots along the western boundary of the Loppa High, we found that these solutions seem to underlie tilted basement blocks, aligned along two lines from the main fault; the first at 10.000 m and the second at 22.000 m (horizontal distance from the left margin of the profile). Integrating the structural information with the EDS plot helps to show that the eastward alignment outlines the Polhem Subplatform, whereas the westward alignment plots directly above tilted blocks recognised during the seismic interpretation.

The relatively shallow Moho below the Bjørnøya Basin is in agreement with the interpretation, that the rifting of this possible aulacogen basin started in the Late Palaeozoic (*Larsen et al., 2005*) and has, since then, maintained isostatic equilibrium during subsequent episodes of crustal thinning.

We think that the curved pattern of the shallowest normal faults linked to the formation of the deep Bjørnøya Basin involves the existence of a major detachment part of the Bjørnøyrenna Fault Complex beneath the Bjørnøya Basin. The possible existence of such a detachment was first proposed by *Gabrielsen et al. (1997)*. The density modelling (Fig. 4) underlines the fact that material of high density, from 2.9 to 3.0 g/cm³, is present at a relatively shallow depth compared to the surrounding area. Putting some high-density material along a major detachment, and interpreting the folded basement reflectors along the Bjørnøyrenna Fault Complex as an imprint of metamorphic gradient, supports the interpretation of a gneiss dome, which would be, in our case, developed coevally with the development of the Bjørnøyrenna Fault Complex. We do not know the initial age of such a detachment, but note that where detachments can be followed from the mainland and onto the shelf offshore the Central and North Norway, they generally originated as part of the Late Caledonian collapse of the mountain range during the Devonian-Early Carboniferous time (*Gabrielsen et al., 1990*), forming major low-angle structures that guide the location of younger detachments that develop during extension and basin formation. By analogy, we suggest that the spatial distribution of the “old” basins in the western Barents Sea may actually be guided by Late Caledonian detachments.

Along a neighbouring profile, *Gudlaugsson et al. (1998)* noticed that the appearance of intra-basement reflectors changes within the Loppa High. Close to the western boundary the reflectors seem to follow an antiform developing parallel to the high-density bulge, whereas toward the west the reflectors are flat. The position of the limit between reflector families could correspond to the limit between lithology, particularly to the median basement block with the highest density. Unfortunately, on seismic, there is no evidence of a structural boundary between the two kinds of reflectors and in seismic, a vertical structure is hard to recognize. If the limit is not structurally controlled, could it be a metamorphic boundary?

Regarding its geometry (clear detachment, suprabasin developed), the gneiss dome system thus modelled could correspond to the description of *Vandherhaeghe et al. (1999)* who stated that gneiss domes can develop by diapiric ascent of partially molten crust during orogenic collapse. As mentioned, the collapse of the Caledonian orogeny in the Devonian-Early Carboniferous is the most likely candidate for triggering the development of the gneiss dome. Its development was probably syntectonic to the propagation of a main detachment in a strong extensional regime like the one that occurred during the Carboniferous time in this region.

Apart from the complexity brought by the gneiss dome, the model proposed a regular Middle Crust thickness of 10 km beneath the Loppa High. Below the Bjørnøya Basin this thickness decreased to 3 km. According to this model, the thinning ratio was at least 0.4. This excessive value encourages us to trust a model incorporating a deep crustal feature such as the proposed gneiss dome.

6. Conclusion and outlook

After the processing that involved extracting the long-wavelength signal (from crustal rocks), the modelling of free air gravity and magnetic data, constrained as far as possible by structural information from seismic data, provides information on the deep structures and poorly imaged intra-basement structures.

The geological model along the chosen profile shows that the combination of a gneiss dome and the separation of three types of basement units

can explain the potential field anomalies. Focusing on the positive gravity anomaly developed along the western boundary of the Loppa High, it was revealed that material of high density (2.9 to 3.0 g/cm³) most likely occurs beneath the Bjørnøyrenna Fault Complex causing a convexity of the Middle and Lower Crust that is interpreted as a metamorphic core complex (gneiss dome) emplacement. Along the same profile, the basement has been divided into three lithological units. The petrophysical database established from measurements on rock samples from Finnmark leads us to interpret the eastern block as a mafic Precambrian unit and the western block as a felsic Precambrian unit. Because of its relatively low susceptibility, the central Precambrian unit is probably composed of an intermediate lithology, i.e., a mixture of felsic and mafic elements.

Using a constant susceptibility within the eastern Precambrian block, we find out the top basement topography rebounded sufficiently to create the depressions observed within the magnetic curve between AM2 and AM3. Thus the fact that this block produces two distinct anomalies is related to its topography. This fits the plot of the EDS computed from the magnetic data using a SI of 0 and a large WS, which outlines only one change in the magnetic properties within the Loppa High basement rocks; and this change corresponds with the central felsic and mafic Precambrian block.

Further work will need to focus on delimiting the extension of the gneiss dome towards both the north and the south. More work is also required to investigate the potential field anomalies from North Norway (Troms and Finnmark) and their potential association with the offshore anomalies using petrophysical, velocity, and reflection seismic data. This will possibly allow us to interpret the structure of the remnants of the Barents Sea Caledonian orogen that lies within the area. However, the preliminary work has already provided some interesting insights into the basement structure of the SW Barents Sea.

Acknowledgments. The study is part of the PETROMAKS project “Basement Heat Generation and Heat Flow in the western Barents Sea – Importance for hydrocarbon systems” which is funded by NFR (Norwegian Research Council), Statoil and NGU. We thank Statoil for allowing us to use seismic data and J. Ebbing, O. Olesen and David Roberts who helped with the text. We also thank our Statoil contacts Arild Ingebrigtsen, Geir Elvebakk and Øyvind Steen for fruitful cooperation.

References

- Blakely R. J., Connard G. G., 1989: Crustal studies using magnetic data, in Geophysical framework of the continental United States: Geological Society of America Memoir 172 p.
- Blakely R. J., 1995: Potential theory in gravity & magnetic applications: Cambridge University Press, New York, 441 p.
- Breivik A. J., Faleide J. I., Gudlaugsson S. T., 1998: Southwestern Barents Sea margin: late Mesozoic sedimentary basins and crustal extension. *Tectonophysics*, **293**, 1, 21–44.
- Breivik A. J., Mjelde R., Grogan P., Shimamura H., Murai Y., Nishimura Y., Kuwano A., 2002: A possible Caledonide arm through the Barents Sea imaged by OBS data. In: Thybo H., (Ed.), Deep seismic probing of the continents and their margins. *Tectonophysics*. **355**, 67–97.
- Breivik A. J., Mjelde R., Grogan P., Shimamura H., Murai Y., Nishimura Y., 2003: Crustal structure and transform margin development south of Svalbard based on ocean bottom seismometer data. *Tectonophysics*, **369**, 37–70.
- Bungum H., Ritzmann O., Maercklin N., Faleide J. -I., Mooney W. D., Detweiler S. T., 2005: Three-Dimensional Model for the Crust and Upper mantle in the Barents Sea Region. *EOS*, **86**, 16, 160–161.
- Campbell D. L., 1983: BASIC Programs to Calculate Gravity and Magnetic Anomalies for 2-1/2 – Dimensional Prismatic Bodies, U.S.G.S. Open-File Report 83–154.
- Clark S. P., 1966: Handbook of physical constants: Geological Society of America Memoir, **97**, 415–436.
- Doré A. G., 1991: The structural foundation and evolution of Mesozoic seaways between Europe and the Arctic. *Palaeogeography, Palaeoclimatology, Palaeoecology*, **87**, 441–492.
- Doré A. G., Gage M. S., 1987: Crustal alignments and sedimentary domains in the evolution of the North Sea, north-east Atlantic margin and Barents shelf. In: Brooks J., Glennie L. (Eds.), *Petroleum Geology of Northwest Europe*. Graham and Trotman, London, 1131–1148.
- Gabrielsen R. H., Færseth R. B., Jensen L. N., Kalheim J. E., Riis F., 1990: Structural elements of the Norwegian continental shelf. Part I: The Barents Sea Region. *Norwegian Petroleum Directorate Bulletin*, **6**, 33 p.
- Gabrielsen R. H., Grunnaleite I., Rasmussen E., 1997: Cretaceous and Tertiary inversion in the Bjørnøyrenna Fault Complex, south-western Barents Sea. *Marine and Petroleum Geology*, **14**, 165–178.
- Geosoft, 2006: Oasis Montaj, Gravity & Magnetic Interpretation v6.1: Euler 3D deconvolution (Processing, Analysis and Visualization System for 3D inversion of Potential Field Data); and GMSYS, Geosoft Incorporated (Online Manuals and Tutorials).
- Gudlaugsson S. T., Faleide J. I., Johansen S. E., Breivik A. J., 1998: Late Palaeozoic structural development of the southwestern Barents Sea. *Mar. and Petrol. Geology*, **15**, 73–102.

- Larsen G. B., Elvebakk G., Henriksen L. B., Kristensen Stein-E., Nilsson I., Samuelsen T. J., Svånå T. A., Stemmerik L., Worsley D., 2005: Upper Palaeozoic lithostratigraphy of the southern part of the Norwegian Barents Sea. *Norges Geologiske Undersøkelse Bulletin*, **444**.
- Nabighian M. N., Grauch V. J. S., Hansen R. O., LaFehr T. R., Li Y., Peirce J. W., Phillips J. D., Ruder M. E., 2005: The historical development of the magnetic method in exploration. *Geophysics*, **70**, 6, 33–61.
- Olesen O., Roberts D., Henkel H., Lile B. L., Torsvik T. H., 1990: Aeromagnetic and gravimetric interpretation of regional structural features in the Caledonides of West Finnmark and North Troms, northern Norway, *Norges Geologiske Undersøkelse Bulletin*, **419**, 1–24.
- Olesen O., Torsvik T. H., Tveten E., Zwaan K. B., Løseth H., Henningsen T., 1997: Basement structure of the continental margin in the Lofoten-Lopphavet area, northern Norway: constraints from potential field data, on-land structural mapping and palaeomagnetic data. *Nor. Geol. Tidsskr.* **77**, 15–33.
- Reid A. B., Allsop J. M., Ganser H., Millet A. J., Somerton I. W., 1990: Magnetic interpretation in three dimensions using Euler deconvolution: *Geophysics*, **55**, 80–91.
- Sigmond E. M. O., 1992: Bedrock map of Norway and adjacent ocean areas. Scale 1:3 million. *Geology of Norway*.
- Skilbrei J. R. 1991: Interpretation of depth to the magnetic basement in the northern Barents Sea (south of Svalbard). *Tectonophysics*, **200**, 127–141.
- Skilbrei J. R., 1995: Aspects of the geology of the southwestern Barents Sea from aeromagnetic data. *NGU Bulletin* 427, 64–67.
- Skilbrei J. R., Skyseth T., Olesen O., 1991: Petrophysical data and opaque mineralogy of high grade and retrogressed lithologies: Implications for the interpretations of aeromagnetic anomalies in northern Vestranden, Western Gneiss Region, central Norway. P. Wasilewski & P. Hood (Eds.) *Magnetic anomalies - land and sea. Tectonophysics*, **192**, 21–31.
- Skilbrei J. R., Kihle O., Olesen O., Gellein J., Solheim D., Nyland B., 2000: Gravity anomaly map, Norway and adjacent ocean areas, Scale 1:3 million, *Norges geologiske undersøkelse*.
- Skilbrei J. R., Olesen O., Osmundsen P. T., Kihle O., Aaro S., Fjellanger E., 2002: A study of basement structures and onshore-offshore correlations in Central Norway. *Norwegian Journal of Geology*, **82**, 263–279.
- Thompson D. T., 1982: EULDPH: a new technique for making computer-assisted depth estimates from magnetic data. *Geophysics*, **47**, 31–37.
- Tsikalas F., 1992: A study of seismic velocity, density and porosity in Barents Sea wells (N. Norway). Unpublished Master Thesis Department of Geology, University of Oslo, Norway.
- Vanderhaeghe O., Teysier C., Wysoczansky R., 1999: Structural and geochronological constraints on the role of partial melting during the formation of the Shuswap metamorphic core complex at the latitude of the Thor–Odin dome, British Columbia. *Canadian Journal of Earth Sciences*, **36**, 917–943.

Ziegler P. A., 1989: Evolution of Laurentia. Kluwer, Dordrecht, 102 p.